

Influence of the Test Method in the Assessment of Concrete Sensitivity to Explosive Spalling

Francesco Lo Monte¹, Roberto Felicetti¹, Alberto Meda² and Anna Bortolussi³

¹ Politecnico di Milano, Milan (Italy)

² Università degli Studi di Roma Tor Vergata, Rome (Italy)

³ Bekaert Maccaferri Underground Solutions, Aalst - Erembodegem (Belgium)

ABSTRACT

In the design phase of structures for which explosive spalling is a critical issue, preliminary screening of concrete mixes plays a key role in pursuing the optimal compromise between costs and efficacy. Generally, the best way to limit or even prevent concrete spalling in structures exposed to fire is to properly define the mix design, especially in terms of fibre type and content. Within this context, in the experimental assessment of spalling sensitivity, it should be kept in mind that there are many influencing aspects, such as specimen geometry, heating curve and possible loading level. All these factors should be accurately defined in order to obtain results representative of the actual service conditions. In the present study, three different test setups have been adopted for the evaluation of spalling sensitivity of two concrete mixes ($f_{cm} = 45$ and 50 MPa) containing different amounts of polypropylene fibre. The testing procedures include: (I) 1m side cubes directly exposed to a localized jet flame (*hot spot test*), (II) 0.8x0.8x0.1 m slabs heated at the intrados under a constant membrane compression (*biaxial loading test*), and (III) a loaded tunnel lining segment exposed to RWS fire curve (*full-scale test*). These methods entail an increasing experimental burden and different levels of detail in the monitored parameters. In the paper, the different typologies of tests are discussed by comparing experimental and numerical results in order to highlight the main influencing factors.

KEYWORD: biaxial loading, explosive spalling, fibre, fire, full-scale test, heating curve, high temperature, hot spot, test method, stress state.

INTRODUCTION

Fire and high temperature represent very severe loading conditions for strategic infrastructures such as tunnels, this making of primary importance the proper evaluation of their fire performance. High temperature, in fact, is detrimental for the structural behaviour due to both the decay of mechanical properties and the introduction of indirect actions. In particular, very high maximum temperatures can be reached in tunnels, even higher than 1000°C for the most severe scenarios [1].

Thanks to incombustibility and thermal insulation capability, concrete members can guarantee satisfactory mechanical behaviour even at such high temperature, provided that spalling phenomenon is limited. The violent detachment of shards from the exposed face typical of concrete during rapid heating, in fact, can lead to the direct exposure of the reinforcing bars to the flames, this dramatically speeding up the loss of bearing capacity.

As is well known, spalling strongly depends on two main triggering factors: (1) stress caused by external loads and thermal gradients, and (2) pore pressure due to water vaporization. Fracture tests carried out on heated concrete cubes ($L = 100$ mm) under sustained pore pressure clearly showed that the combination of pressure and stress is necessary for spalling occurrence [2].

Due to fast heating and low thermal diffusivity of concrete, significant temperature gradients arise, this leading to thermal stress profiles characterized by compression next to the exposed face and tension in the colder core (both parallel to the isothermal surfaces). In particular, compressive stress fosters cracking, locally reducing the mechanical stability. On the other hand, pore pressure rises due to water vaporization and contributes to a violent propagation of cracks, typical of spalling phenomenon. Pressure gradients push moisture toward the inner core, where moisture content can increase and even lead to saturation (the so-called moisture clog). High-Performance Concretes (HPC) are prone to moisture clog formation due to their very low permeability, and pore pressure up to 4 MPa can be achieved [3,4]. This makes HPC rather sensitive to spalling [3,5].

As it is well known, the most efficient way to strongly reduce the probability of spalling is to properly design the concrete mix, especially with the addition of polypropylene (or hybrid) fibre [3,6]. Cement paste microcracking during polypropylene fibre melting [6-8] leads to smoother moisture gradients [9], lower values of pressure in the pores and, possibly, to an increase of transient thermal strain favouring stress relaxation [7,10].

Even though numerical models dealing with the thermo-hygro-mechanical problem are available in the literature, no direct control is possible on most of the involved material parameters. Hence, experimental investigation is generally preferred for spalling sensitivity assessment, via small-, medium- or full-scale tests, on loaded or unloaded specimens [11].

Many experimental studies in the literature can be classified as small-scale investigations. As examples, in Kalifa (2000) [3], Mindeguia et al. (2010) [12], Toropovs et al. (2015) [9] and Felicetti et al. (2017) [2] both temperature and pressure have been measured in samples experiencing a substantially monodimensional thermo-hygral transient. In Lo Monte and Gambarova (2015) [13] the focus was on corner spalling, where thermal dilation along two converging planes is the dominant fracture mechanism. All tests were performed on unloaded prismatic specimens and relevant spalling never occurred. On the contrary sizeable spalling was observed in small-scale tests carried out in loaded samples (Hertz and Sørensen, 2005 [14]; Tanibe et al., 2011 [15]; Connolly, 1995 [16]).

Medium-scale tests generally consist in slabs or prismatic specimens heated on one side, either in loaded or unloaded conditions. External loading can be applied (1) in just one direction, via pre-/post-tensioning systems (as in Heel and Kusterle, 2004 [17]; Sjöström et al., 2012 [18]; Boström et al., 2007 [19]; Jansson and Boström, 2008 [20]) or active actuators (Carré et al., 2013 [21]; Rickard et al., 2016 [22]), or (2) in two directions via a restraining frame (as in Connolly, 1995 [16]; Heel and Kusterle, 2004 [17]) or by means of hydraulic jacks (Lo Monte and Felicetti, 2017 [10]). The common evidence is that spalling sensitivity increases from unloaded to loaded specimens, and from uniaxial to biaxial loading conditions (Miah et al., 2016 [13]).

Finally, full-scale investigations consist in testing structural members or substructures under restraining and loading conditions representative of the real ones.

In the design phase of spalling-sensitivity structures, preliminary screening of concrete mixes is an important issue in order to obtain the optimal compromise between costs and efficacy, and, to this aim, the choice of the proper scale of testing is very important. Full-scale test, for example, is the most representative for the real conditions, but is costly and time demanding, hence unsuitable for a first categorization of several concrete mixes. On the opposite, small-scale tests on unloaded samples can be too far from the service conditions of the structural member at issue, hence not representative of the effective behaviour in fire. This comes from the fact that experimental assessment is directly influenced by many aspects such as specimen geometry, heating curve and possible loading level, all factors which govern thermal gradients and stress, concrete permeability evolution and pore pressure development. In this context, three different test setups have been compared for the evaluation of spalling sensitivity and the results are discussed in order to highlight the main influencing factors.

TEST METHODS AND MIX DESIGN

The three different testing procedures compared in the present study include:

- *hot spot test*: 1m side cubes directly exposed to a localized jet flame,
- *biaxial loading test*: 0.8x0.8x0.1 m slabs heated at the intrados under a constant membrane compression,
- *full-scale test*: testing on a tunnel lining segment subjected to external loads.

The three setups imply an increasing experimental demand in terms of costs and time, while providing information with different levels of detail accordingly to the monitored parameters.

Hot spot test

Testing procedure is based on a hot spot (about 250 mm in diameter) applied to one face of a 1m side concrete cube via a 86 kW propane torch (Figure 1). The temperature, monitored by means of a small plate thermometer, reaches instantly the target value (defined as 800°C in the present case) and then is kept constant for the whole test duration. Only spalling depth at the end of heating is measured. No external load is applied, hence stress is caused by thermal gradients only.

This testing procedure is very cheap, rapid and of easy implementation. The uncommon geometry of the sample is dictated by the fact that very often 1m side mountable formworks are available at pre-casting plants for collecting spare concrete. Considering that concrete volume is not an issue in tunnel segments production, casting 1m³ specimens is affordable and allows several test faces. On the other hand, having larger samples than the hot spot diameter is an advantage in spalling sensitivity testing, since the restraint exerted by cold concrete against the thermal dilation of the heated region is very effective. This leads to relevant thermal stress, as required for highlighting possible spalling susceptibility.

Biaxial loading test

An experimental setup has been recently developed at Politecnico di Milano to investigate concrete sensitivity to explosive spalling. The setup allows to perform hot tests on biaxial loaded slabs under strictly controlled boundary conditions [10]. Specimens consist in slabs (800x800x100 mm, Figure 2) exposed to standard fire curve at the intrados via a horizontal furnace powered by an actively controlled propane burner. During heating, a constant biaxial compression can be applied in the range $\sigma_{\text{mean}} = 0\text{-}15$ MPa thanks to eight hydraulic jacks. Biaxial membrane loading is implemented in order to emphasize the effect of compression and hydraulic jacks are preferred to passive techniques based on restrained thermal strain, since in the latter case compression varies during heating due to the effect of thermal dilation on both the slab and the restraining system.

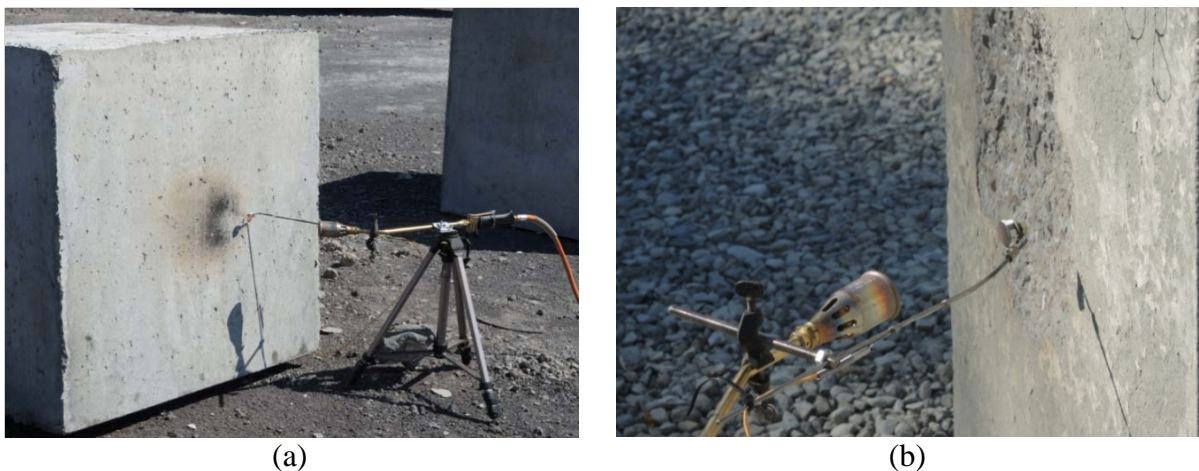


Figure 1. *Hot spot test*: (a) concrete cube exposed to a jet flame, and (b) detail of the heating system.

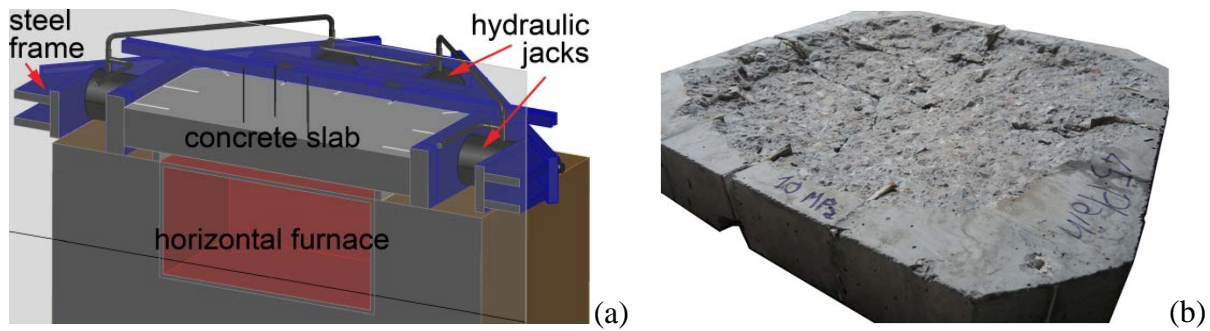


Figure 2. **Biaxial loading test:** (a) section of the concrete slab within the loading system placed over the horizontal furnace, and (b) picture of a spalled slab after the test.

Slab vertical deflection is monitored via 6 displacement transducers. Even though not measured in the present case, also temperature and pore pressure can be monitored within the specimen if sensors are fitted during casting. The described setup allows to control the main parameters involved such as heating curve and external load, thus leading to a clearer understanding of the results.

Full-scale test

In full-scale tests, the real structural member is tested under restraining and loading conditions very close to the actual service ones. In the present case, one test has been performed at the Leipzig Institute for Materials Research and Testing – MFPA (Work Group 3.2 - Fire Behaviour of Building Components and Special Constructions). A tunnel lining segment (length = 3.43 m, width = 1.80 m and thickness = 0.55 m) is loaded vertically in three points and horizontally in one direction by means of hydraulic jacks, according to the scheme reported in Figure 3. Load is applied before heating and then kept constant. Fire load is applied at the bottom face only according to the RWS (Rijks-waterstaat) fire curve. During heating horizontal and vertical displacements at the actuators are monitored, together with the temperature within the thickness.

Due to high time and costs required, such experimental procedure cannot be used for screening different concrete mixes, but just for the final validation of the designed concrete in restraining, loading and heating conditions very close to the real ones.

Mix design and experimental program

The above-described tests have been carried out for spalling sensitivity assessment of two concrete mixes ($f_{cm} = 45$ and 50 MPa) containing different amounts of polypropylene ($L = 6$ mm, $\varnothing = 18$ μm and melting point $T = 165^\circ\text{C}$) and steel (hook end, $L = 60$ mm and $\varnothing = 750$ μm) fibres, for a total number of 8 mixes. Hot spot test was performed on all concretes, while mixes with 2.0 kg/m^3 of polypropylene fibre were excluded for biaxial loading tests, since the results on 1m side cubes showed that 1.5 kg/m^3 of polypropylene fibre was enough to prevent spalling. Finally, full scale test was performed on one mix only, for final validation. In Table 1 the main features of concrete mixes and the tests carried out on each of them are schematically reported.

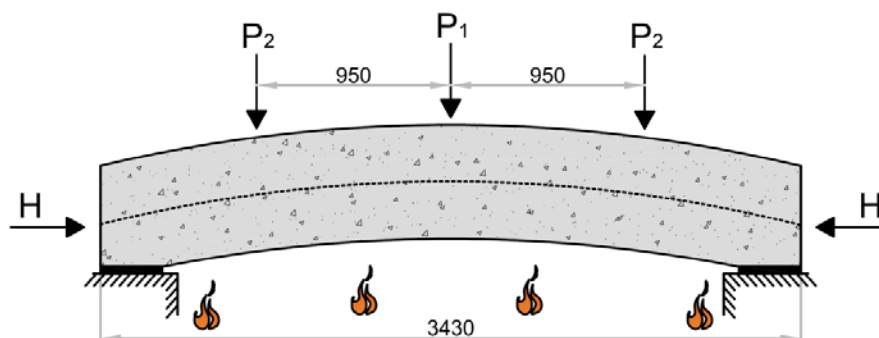


Figure 3. **Full-scale test:** scheme of loading and heating of a tunnel lining segment.

Table 1. Concrete mixes and tests plan.

mix	f_{cm} [MPa]	pp fibre [kg/m ³]	steel fibre [kg/m ³]	hot spot test	biaxial loading test	Full-scale test
45_Plain	45	-	-	X	X	X
45_1.5		1.5	-	X	X	
45_2.0		2.0	-	X		
45_1.5_4D		1.5	40	X	X	
50_Plain	50	-	-	X	X	
50_1.5		1.5	-	X	X	
50_2.0		2.0	-	X		
50_1.5_4D		1.5	40	X	X	

EXPERIMENTAL RESULTS

Hot spot test

In Figure 4a all specimens ready for hot spot test in the construction site are shown. In Figure 4b the experimental temperature measured at the small plate thermometer during heating is reported for each test, together with standard and RWS fire curves. Due to the working conditions, temperature sizably fluctuated, even though the average value is very close to the target value of 800°C. Test duration was set to 15 min, since it was sufficient for highlighting spalling sensitivity. Spalling was observed only in the two plain mixes, 45_Plain (Figure 5a) and 50_Plain, starting at 45 and 60 s, with final maximum spalling depth of 100 and 120 mm, respectively.

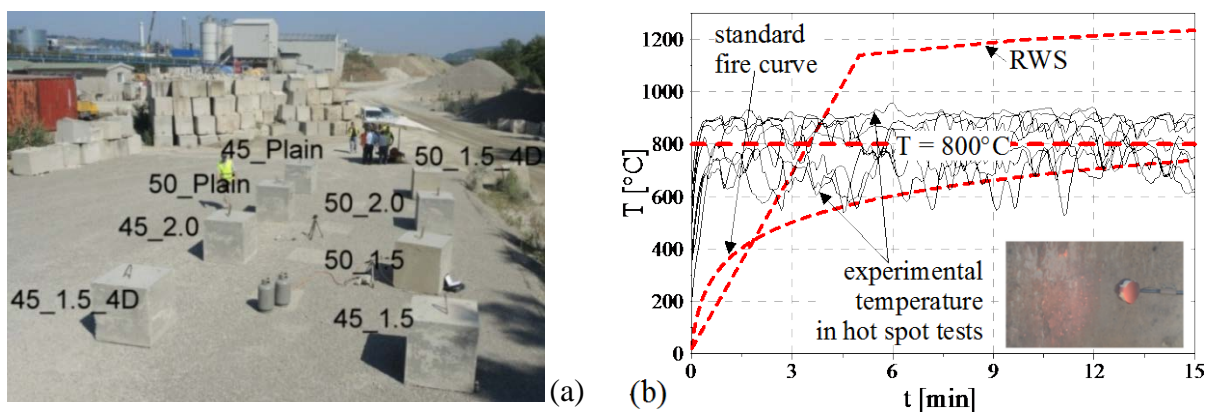


Figure 4. (a) Specimens for hot spot tests in the construction site, and (b) comparison among experimental temperature measured at the small plate thermometer, target temperature, standard fire curve and RWS.



Figure 5. Specimens at the end of the hot spot test: (a) mix 45_Plain and (b) mix 45_1.5.

In the mixes with 1.5 kg/m³ of polypropylene fibre (45_1.5 and 50_1.5) test duration was 30 min so to check possible late spalling. In Figure 5a the typical spalling surface after testing is shown (mix 45_Plain), while in Figure 5b mix 45_1.5 after testing is depicted, where no spalling or even scaling was observed. All test results are summarized in Table 2.

Biaxial loading test

In Figure 6a the comparison between standard fire curve and temperature measured at the plate thermometer inside the furnace is reported for all tests. As it can be noted, the prescribed temperature is strictly followed thanks to the active control system of the propane burner. Tests have been performed under an external biaxial compression of 10 MPa, so to simulate the working condition in the 100 mm close to the surface of the tunnel lining.

Spalling occurred only in plain mixes, 45_Plain and 50_Plain, after 17 and 15 min, respectively. As shown in Figure 7a, spalling progression involves all the heated area with a final average/maximum depth of 55/60 and 62/69 mm for 45_Plain and 50_Plain, respectively. On the other hand, no spalling was observed in concretes with polypropylene fibre.

In Figure 6b the vertical displacement at the mid-span point is plotted as a function of time. No remarkable difference can be noted between plain concretes, while if polypropylene fibre is added, sagging deflection is sizably reduced. This can be ascribed to the larger increase of concrete deformability with temperature in the latter case, probably due to diffuse damage and higher transient thermal strain occurring when polypropylene fibre is added [7,10].

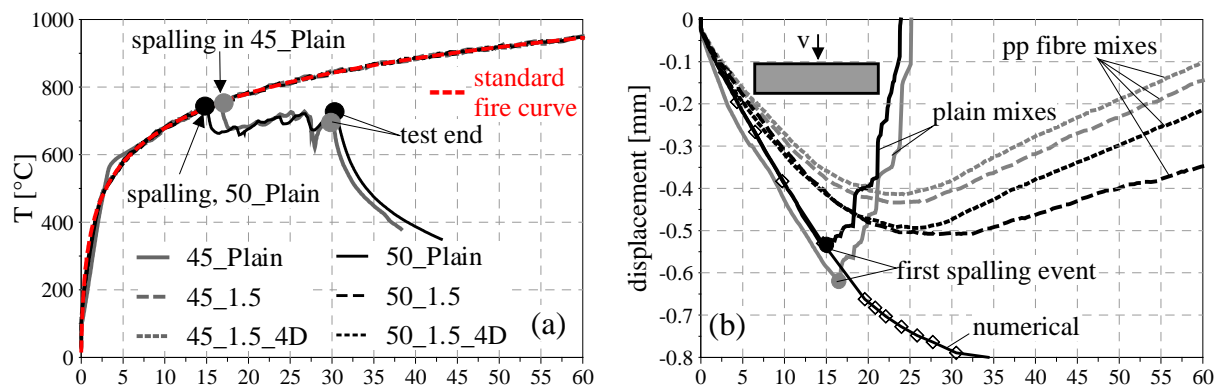


Figure 6. (a) Temperature measured at the plate thermometer inside the oven and standard fire curve, and (b) vertical mid-span displacements (positive upwards).

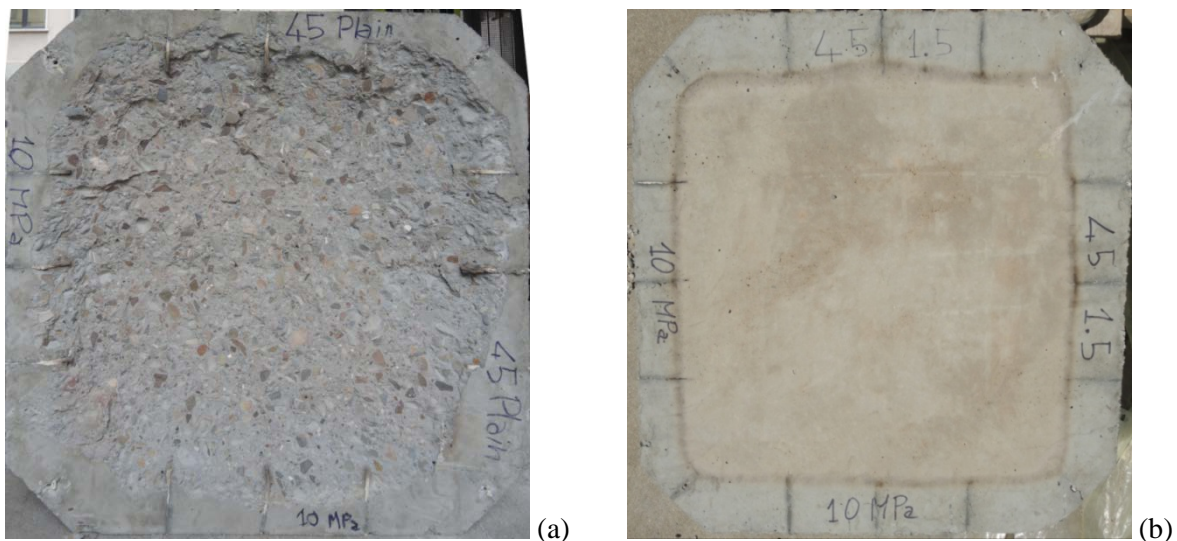


Figure 7. Specimens at the end of the biaxial loading test: (a) mix 45_Plain and (b) mix 45_1.5.

Full-scale test

Full-scale test is performed on one loaded tunnel lining segment ($l \times w \times t = 3.43 \times 1.80 \times 0.55$ m) made in concrete without fibre (mix 45_Plain), heated at the bottom face according to RWS fire curve. Load is applied according to the scheme of Figure 3, with $P_1 = 593$ kN, $P_2 = 297$ kN and $H = 5300$ kN, with the aim of simulating the service life conditions. Load was applied before heating and then kept constant during the test. In Figure 8a the comparison between RWS fire curve and temperature measured inside the furnace is shown, proving a rather good agreement. Spalling started after 3 min of heating with a final average/maximum depth of 154/474 mm, involving the whole exposed face, as evident in Figure 9. Local peaks may have been fostered by some grouted holes for thermocouple installation. It is worth noting that the temperature reached during the test are so high that concrete and reinforcing bars start melting after about 45 min of heating. In Figure 8b the horizontal and vertical displacements at the actuators are plotted as functions of time.

NUMERICAL ANALYSES AND DISCUSSION

For the sake of comparison, the main features and results of all tests are collected in Table 2, clearly showing that the three setups lead to different outcomes in terms of spalling onset time and final depth. In order to try to explain such differences, numerical analyses have been performed aimed at computing the stress state in the specimens in a significant time range including the onset of spalling, so to understand if there are common triggering conditions. It is worth noting that the qualitative results of the test setups (especially hot spot and biaxial loading tests) provide consistent information about the efficacy of the introduction of polypropylene fibre (even in combination with steel fibre) in preventing spalling.

Numerical simulations have been performed by using the finite element code Abaqus. Thermal properties according to EC2 [24] are adopted: lower curve for the thermal conductivity, specific heat for negligible moisture content and initial density of 2300 kg/m^3 .

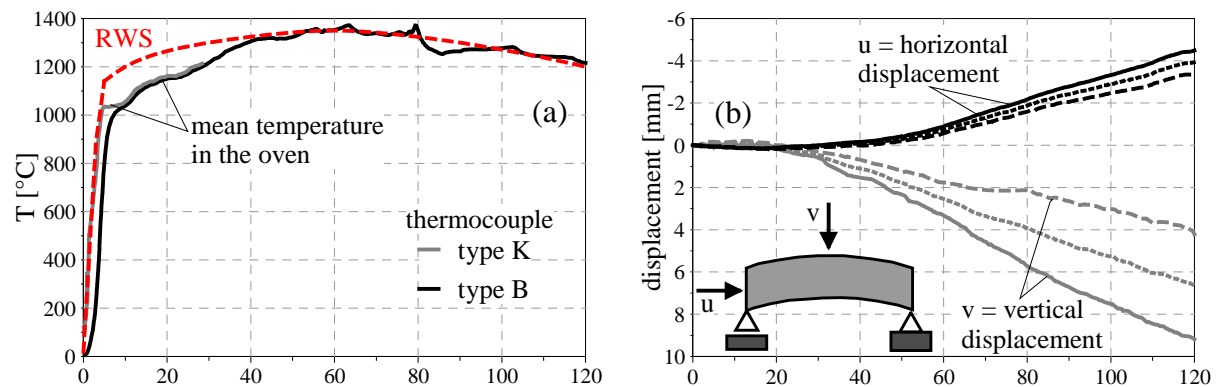


Figure 8. (a) Temperature measured at the plate thermometer inside the oven and RWS fire curve, and (b) vertical/horizontal displacement at the actuators.



Figure 9. Heated (bottom) face of the tunnel lining segment after testing.

Concrete Damaged Plasticity model is used for concrete mechanical behaviour. The variation with temperature of compressive and tensile strengths is defined as suggested in EC2 [24], while fracture energy in virgin conditions G_f^{20} is evaluated according to Model Code '90 [25] and then kept constant with temperature ($G_f^T = G_f^{20} = 0.117 \text{ N/mm}$), since this last parameter is far less heat-sensitive compared to the other concrete mechanical properties [26]. Stiffness and thermal expansion are calibrated in order to obtain results representative of the experimental tests in terms of initial rate and maximum value of mid-span deflection (see Figure 6b). In Figure 10, normalized decay of compressive and tensile strengths, stiffness and fracture energy are reported together with thermal expansion variation ($f_c^{20} = 45 \text{ MPa}$, $f_{ct}^{20} = 3.3 \text{ MPa}$, $E_c^{20} = 34 \text{ GPa}$). Concerning stress-strain relationships, a bilinear behaviour is implemented in tension, while in compression the curve suggested by EC2 [24] is used (as in [27]), where peak strain is defined as $\varepsilon_{c1}^T = 1.5 f_c^T / E_c^T$ so as to match the initial material stiffness (see also [2,10]).

As regards steel reinforcement, which was present only in the tunnel lining segment for the full-scale test, thermo-physical and mechanical properties have been implemented according to EC2 [24] (as in [27]). The *Plasticity* model of Abaqus has been used.

In Figure 11 the numerical thermal profiles along the central axis are shown for each specimen geometry, in the 150 mm next to the exposed face (*ref. line* in the inserts of Figure 11). It is evident as the temperature evolution is rather different among the test setups because of the adoption of distinct heating curves. On the contrary, it is interesting to observe as in the three tests, spalling (if any) occurs when temperature in the hot face is in between 300 and 350°C. It is also worth noting that temperature gradients in hot spot and full-scale tests are very similar at spalling onset (namely, about 1 and 3 min of heating, respectively).

Table 2. Summary of test results.

Mix	hot spot test			biaxial loading test			full-scale test		
	Fire duration [min]	Spalling initiation [min]	max spalling depth [mm]	Fire duration [min]	Spalling initiation [min]	avg/max spalling depth [mm]	Fire duration [min]	Spalling initiation [min]	avg/max spalling depth [mm]
45_Plain	15	1.00	100	30	17	55/60	120	3	154/474
45_1.5	30	-	-	60	-	-			
45_2.0	15	-	-	-	-	-			
45_1.5_4D	15	-	-	60	-	-			
50_Plain	15	0.75	120	30	15	62/69			
50_1.5	30	-	-	60	-	-			
50_2.0	15	-	-	-	-	-			
50_1.5_4D	15	-	-	60	-	-			

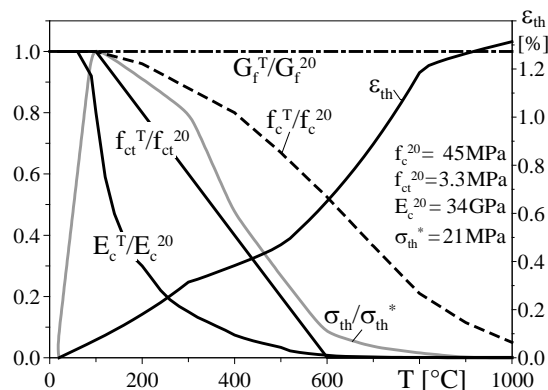


Figure 10. Normalized decay of compressive and tensile strengths, stiffness and fracture energy together with thermal expansion used in numerical analyses. σ_{th} is the thermal stress in perfectly restrained conditions ($\sigma_{th} = E_c^T \cdot \varepsilon_{th}$).

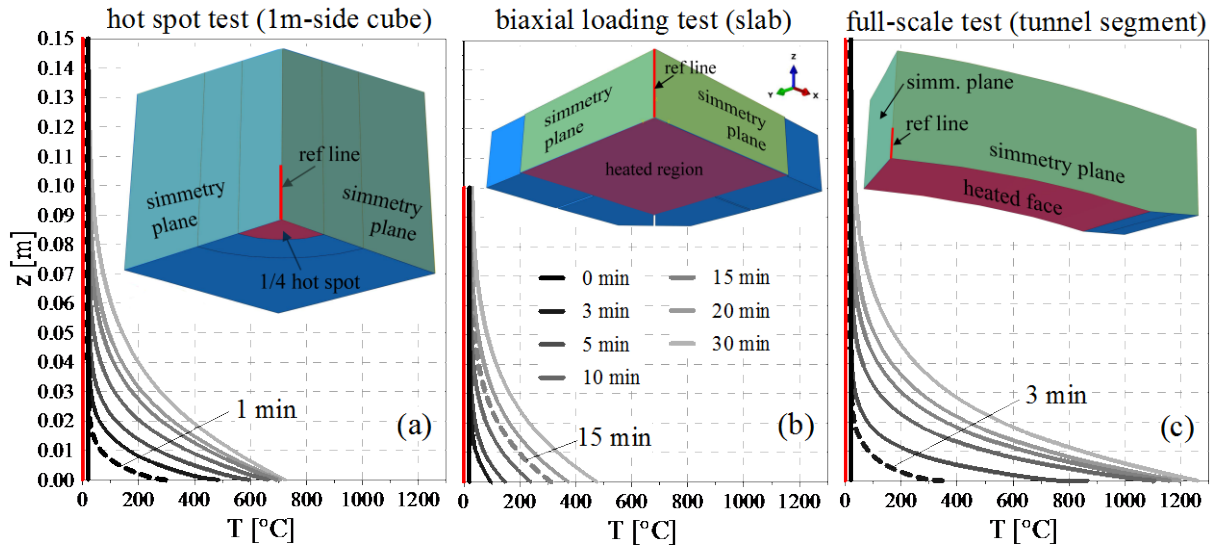


Figure 11. (a-c) Thermal profiles at mid-span section of the specimen for the three tests.

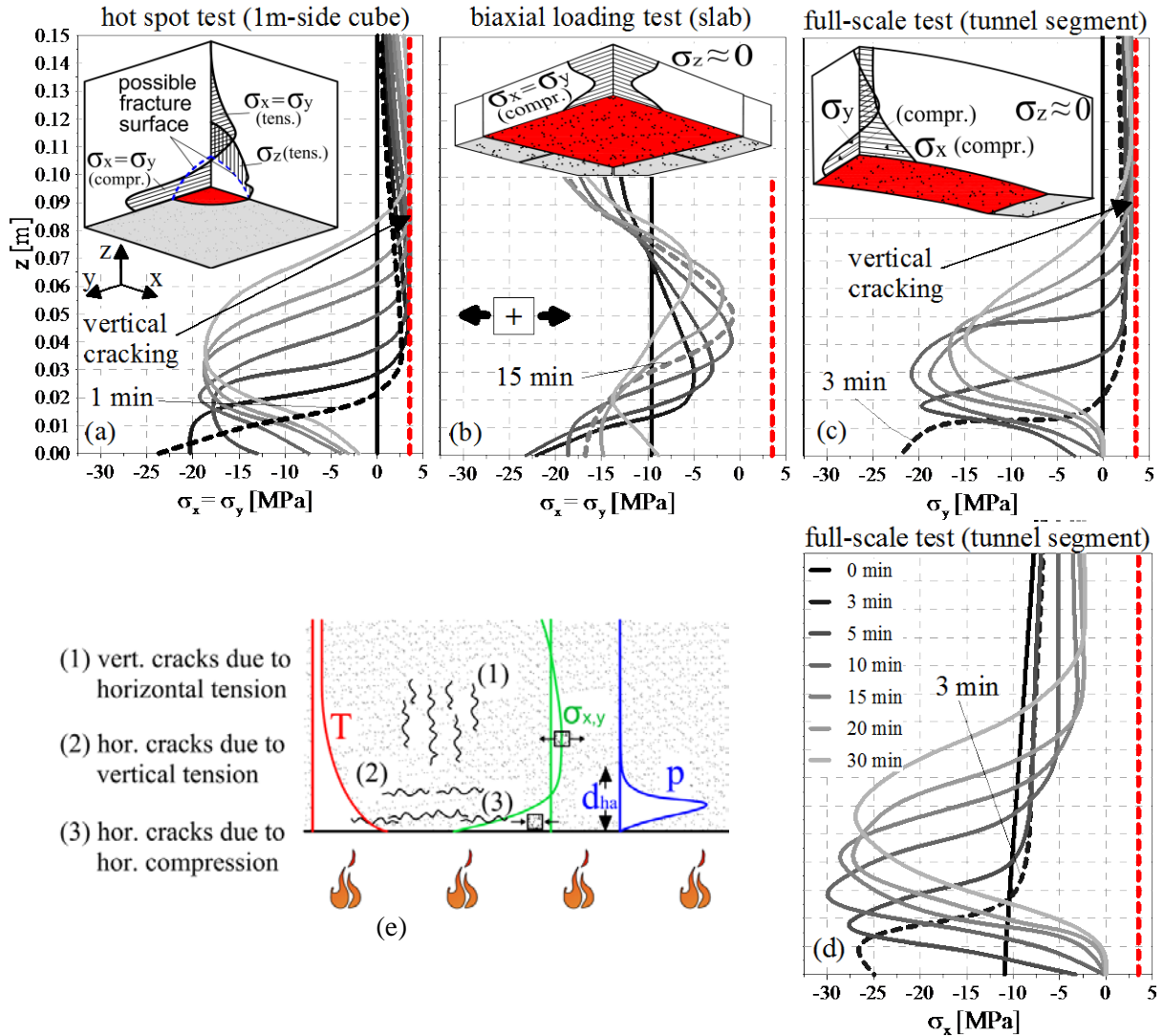


Figure 12. (a-d) Stress profiles at mid-span section of the specimen in the three tests, and (e) crack patterns in a concrete member exposed to fire. Stresses σ_x and σ_y are parallel to the exposed face.

Numerical stress profiles in the same segment (*ref. line* in the inserts of Figure 11) and for the same time steps shown for temperature profiles are reported in Figure 12a-d. Stresses σ_x and σ_y are parallel

to the exposed face and, obviously, $\sigma_x = \sigma_y$ for both hot spot and biaxial loading tests due to the double symmetry of both heating and loading. On the other hand, in full-scale test, σ_x comes from the interaction between thermal gradients and external loads, while σ_y is caused by thermal gradients only (hence, $\sigma_x \neq \sigma_y$). Finally the stress normal to the exposed face, σ_z , is almost negligible in biaxial loading and full-scale tests, since heating flux is essentially unidimensional, while tension – even approaching concrete tensile strength – arise in the hot spot test, as sketched in the insert of Figure 12a.

In Figure 12e the possible crack patterns in a concrete member exposed to fire at the bottom face are depicted. Horizontal thermal stress develops because of the steep thermal gradients, leading to compression next to the exposed face and tension in the colder core. Compressive stress in the hot layers fosters cracking parallel to the isothermal surfaces (crack pattern (3) in Figure 12e), locally reducing the mechanical stability, while tension can trigger orthogonal cracking (crack pattern (1) in Figure 12e). Stress normal to the exposed face becomes sizable when isotherms are significantly curved, as occurs at the edges of the hot spot, leading to the formation of a fracture surface as sketched in the insert of Figure 12a (crack pattern (2) in Figure 12e).

Looking at Figure 12a it can be expected that, in hot spot test, cracking occurs deeper than the hygrally-active region (namely where pore pressure develops, according to Figure 12e), this latter resulting within the compression region. This fosters pressure build-up in the pores. Very similar situation occurs in the full-scale test along the generatrix (y axis), while in the circumferential direction (x axis) compression is even higher due to the external loads. Finally, in biaxial loading test, no tension at all takes place due to the external membrane compression.

Even though the stress profiles are quite different for biaxial loading test, the order of magnitude of the maximum compression is close to the other testing setups. The different stress state comes from (1) the lower specimen thickness and (2) the slower heating curve. Because of the reduced flexural stiffness, in fact, slab bends due to thermal bowing and compression in the hot layers is mildly reduced (with respect to hot spot and full-scale tests, in which specimen is stiffer). Nevertheless, compressive stress higher than 20 MPa is evaluated in the hot layer of the slab in the first minutes of heating. Even higher values could be reached also adopting more severe heating curves, such as RWS.

The critical point, now, is to understand if compressive stress in the range 20-25 MPa is enough to trigger spalling. Assuming that pore pressure can reach a value close to 1 MPa (at about 250°C, average temperature in the hottest layers), the equivalent tensile hydrostatic stress acting on the solid skeleton for a Normal-Strength Concrete is of the same order of magnitude of the pressure itself [2]. Such tension should be added to that induced by thermal gradients and by meso-scale effects (such as kinematic incompatibility between aggregate and cement paste, and the deviation of the compression isolines due to aggregates). It is enough that all these effects lead to an equivalent tension of about 1.5 MPa, that about 50% of the hot tensile strength is attained. According to the commonly used triaxial failure criteria for concrete, this implies that uniaxial compressive strength is reduced by almost 50%, namely $f_c = 0.5 \cdot f_c^{300^\circ\text{C}} \approx 20$ MPa. Biaxial compressive strength can be assumed as the uniaxial one increased by 20%, so obtaining $f_{c,b} = 1.2 \cdot f_c = 24$ MPa. Hence, it can be concluded that compressive stress approaching 20-25 MPa could be enough to trigger spalling, if moderate pressure rises in the pores (in the order of 1 MPa), such result being consistent with the outcome of the three different tests.

CONCLUDING REMARKS

In the present paper the results of three different test setups for the assessment of concrete sensitivity to explosive spalling are discussed. Tests have been carried out within an experimental campaign aimed at screening different concrete mixes for the final application to tunnel lining segments.

In the first phase, spalling behaviour of all mixes have been investigated via a very easy test setup based on 1m side cubes heated on a 25 cm-diameter hot spot on one face. This test proved to be effective in

highlighting spalling sensitivity even though stress is caused by thermal gradients only. Afterwards only 6 of the 8 concrete mixes were selected for the second phase, based on heating unreinforced concrete slabs at the bottom face under biaxial membrane compression, so to investigate the effect of external loading. Finally, the full-scale test on a concrete tunnel lining segment (made with the designed mix) was performed under restraining and loading conditions very close to the real ones. For all the test setups, spalling occurred only in plain mixes (without polypropylene fibre), with rather different values of spalling time onset and final depth. In order to explain such differences and to understand possible common triggering conditions, thermo-mechanical numerical analyses have been performed.

In all cases, first spalling event occurred when the temperature in the hottest 5 mm was between 100 and 350°C (300-350°C at the heated face), thermal range for which sizable pore pressure can be reached. The tensile stress induced by pore pressure, together with tension caused by thermal gradients and meso-scale effects, is expected to lead to an apparent decrease of compressive strength sufficient to instate the conditions for spalling initiation.

It is worth noting that stress profiles along the mid axis of a 1m side cube and of a tunnel lining segment are rather similar, since they are mainly driven by thermal gradients developing in thick members. On the other hand, in biaxial loading test, the lower flexural stiffness allows for thermal bowing this slightly smoothing down the thermal stresses; nevertheless, compression higher than 20 MPa is attained thanks to the application of the external biaxial membrane load and even higher values could be obtained for sharper heating curves.

ACKNOWLEDGEMENTS

The Authors are grateful to Leipzig Institute for Materials Research and Testing – MFPA (Work Group 3.2 - Fire Behaviour of Building Components and Special Constructions) for providing the results regarding the full-scale test on the tunnel lining segment.

REFERENCES

1. FIT, *Technical Report – Part 1: Design Fire Scenarios*, European Thematic Network FIT – Fire in Tunnels , Rapporteur A. Haack, supported by the European Community under the 5th Framework Programme ‘Competitive and Sustainable Growth’ Contract n° G1RT-CT-2001-05017, 2005.
2. Felicetti R., Lo Monte F. and Pimienta P., “A New Test Method to Study the Influence of Pore Pressure on Fracture Behaviour of Concrete during Heating”, *Cement and Concrete Research*, **94**, 13–23, 2017.
3. Kalifa P., Menneteau F. D. and Quenard D., “Spalling and pore pressure in HPC at high temperatures”, *Cement and Concrete Research*, **30**,1915–1927, 2000.
4. Kalifa P., Chéné G., Gallé C., “High-temperature behaviour of HPC with polypropylene fibres. From spalling to microstructure”, *Cement and Concrete Research*, **31**,1487–1499, 2001.
5. Khoury G. A., “Effect of fire on concrete and concrete structures”, *Progress in Structural Engineering and Materials*,**2**, 429–447, 2000.
6. Khoury G. A., “Polypropylene Fibres in Heated Concrete. Part 2: Pressure Relief Mechanisms and Modelling Criteria”, *Magazine of Concrete Research* **60** (3),189–204, 2008.
7. Huismann S., Weise F., Meng B., Schneider U., “Transient strain of high strength concrete at elevated temperatures and the impact of polypropylene fibers”, *Materials and Structures*, **45**, 793–801, 2012.
8. Pistol K., Weise F., Meng B. and Diederichs U., “Polypropylene fibres and micro cracking in fire exposed concrete”, *Advanced Materials Research*, **897**, 284-289, 2014.

9. Toropovs N., Lo Monte F., Wyrzykowski M., Weber B., Sahmenko G., Vontobel P., Felicetti R. and Lura P., “Real-time measurements of temperature, pressure and moisture profiles in High-Performance Concrete exposed to high temperatures during neutron radiography imaging”, *Cement and Concrete Research*,**68**, 166–173, 2015.
10. Lo Monte F. and Felicetti R. “Heated slabs under biaxial compressive loading: a test set-up for the assessment of concrete sensitivity to spalling”, *Materials and Structures*, **50** (192), 2017.
11. Krzemiańska K., Hager I., “Assessment of concrete susceptibility to fire spalling: A report on the state-of-the-art in testing procedures”, *Procedia Engineering*,**108**, 285–292, 2015.
12. Mindeguia J. C., Pimienta P., Noumowé A. and Kanema M., “Temperature, Pore Pressure and Mass Variation of Concrete Subjected to High Temperature – Experimental and Numerical Discussion on Spalling Risk”, *Cement and Concrete Research*,**40**, 477–487, 2010.
13. Lo Monte F., Gambarova P. G., “Corner spalling and tension stiffening in heat-damaged R/C members: a preliminary investigation”, *Materials and Structures*,**48**, 3657–3673, 2015.
14. Hertz K. and Sørensen L., “Test method for spalling of fire exposed concrete”, *Fire Safety Journal*,**40**, 466-476, 2005.
15. Tanibe T, Ozawa M, Lustoza RL, Kikuchi K, Morimoto H., “Explosive spalling behaviour in restrained concrete in the event of fire”. Proceedings of the 2nd International RILEM Workshop on “Concrete Spalling due to Fire Exposure”, Delft (the Netherlands), October 5-7, 319-326, 2011.
16. Connolly R., *The Spalling of Concrete in Fires*, PhD Thesis, University of Aston in Birmingham, 1995.
17. Heel A. and Kusterle W., “Die Brandbeständigkeit von Faser-, Stahl- und Spannbeton [Fire resistance of fiber-reinforced, reinforced, and prestressed concrete]” (in German), Tech. Rep. 544, Bundesministerium für Verkehr, Innovation und Technologie, Vienna, 2004.
18. Sjöström J., Lange D., Jansson R. and Boström L., “Directional Dependence of Deflections and Damages during Fire Tests of Post-Tensioned Concrete Slabs”, *Proc. of the 7th Int. Conf. on Structures in Fire – SIF’12*, June 6-8, 2012, Zurich (Switzerland), 589–598, 2012.
19. Boström, L., Wickström, U., Adl-Zarrabi B., “Effect of Specimen Size and Loading Conditions on Spalling of Concrete”, *Fire and Materials*, **31**, 173-186, 2007.
20. Jansson R. and Boström L., *Spalling of concrete exposed to fire*, SP Technical Research Institute of Sweden, Borås; 2008.
21. Carré, H., Pimienta, P., La Borderie, C., Pereira, F., and Mindeguia, J. C., “Effect of Compressive Loading on the Risk of Spalling”, Proceedings of the 3rd International Workshop on Concrete Spalling due to Fire Exposure, pp. 01007, Paris (France), September 25-27, 2013.
22. Rickard I., Bisby L., Deeny S. and Maluk C., “Predictive Testing for Heat Induced Spalling of Concrete Tunnels - the Influence of Mechanical Loading”, Proceedings of the 9th international Conference “Structures in Fire 2016 – SIF’16), 217-224, Princeton (USA), June 8-10, 2016.
23. Miah, Md. J., Lo Monte, F., Felicetti, R., Carré, H., Pimienta, P., Borderie, C. L., “Fire spalling behaviour of concrete: Role of mechanical loading (uniaxial and biaxial) and cement type”, *Key Engineering Materials*, **711**, 549-555, 2016.
24. EN 1992-1-2:2004, Eurocode 2 - Design of concrete structures - Part 1-2: General rules - Structural fire design, European Committee for Standardization (CEN), Brussels (Belgium), 2004.
25. CEB – FIP Model Code 1990, Comité Euro-International du Béton, Lausanne (Switzerland), 1993.
26. Bamonte P. and Felicetti R., “High-Temperature Behaviour of Concrete in Tension”, *Structural Engineering International*, **4**/2012, 493-499, 2012.
27. Bamonte P. and Lo Monte F., “Reinforced Concrete Columns Exposed to Standard Fire: Comparison among Different Constitutive Models for Concrete at High Temperature”, *Fire Safety Journal*,**71**, 310–323, 2015, DOI: <http://dx.doi.org/10.1016/j.firesaf.2014.11.014>.